Acta Oceanol. Sin., 2024, Vol. 43, No. 4, P. 1–14
https://doi.org/10.1007/s13131-024-2342-7
http://www.aosocean.com
E-mail: ocean2@hyxb.org.cn

Influence of lithospheric thickness distribution on oil and gas basins, China seas and adjacent areas

Jing Ma[1, 2], Wanyin Wang[1, 3, 4*], Hermann Zeyen[2], Yimi Zhang[1, 5], Zhongsheng Li[1], Tao He[1, 5], Dingding Wang[1, 6]

[1] School of Geology Engineering and Geomatics, Key Laboratory of Western China's Mineral Resources and Geological Engineering of Ministry of Education, Chang'an University, Xi'an 710054, China

[2] UMR8148 GEOPS, CNRS/Université Paris-Saclay, Département des Sciences de la Terre, Bât. 504, 91405, France

[3] CNOOC Research Institute Co., Ltd., Beijing 100027, China

[4] Qingdao Institute of marine geology, Qingdao 266071, China

[5] Department of Earth Sciences, Memorial University of Newfoundland, St. John's, Newfoundland AlB3X5, Canada

[6] University of Naples Federico II, Department of Earth Sciences, Naples, 80138, Italy

Received 26 December 2023; accepted 5 February 2024

© Chinese Society for Oceanography and Springer-Verlag GmbH Germany, part of Springer Nature 2024

Abstract

The distribution of oil and gas resources is intricately connected to the underlying structure of the lithosphere. Therefore, investigating the characteristics of lithospheric thickness and its correlation with oil and gas basins is highly important. This research utilizes recently enhanced geological–geophysical data, including topographic, geoid, rock layer thickness, variable rock layer density, and interface depth data. Employing the principles of lithospheric isostasy and heat conduction, we compute the laterally varying lithospheric thickness in the China seas and adjacent areas. From these results, two pivotal parameters for different types of oil and gas basins were statistically analyzed: the minimum lithospheric thickness and the relative fluctuation in lithospheric thickness. A semiquantitative analysis was used to explore the connection between these parameters and the hydrocarbon abundance within the oil and gas basins. This study unveils distinct variations in lithospheric thickness among basins, with oil and gas rich basins exhibiting a thicker lithosphere in the superimposed basins of central China and a thinner lithosphere in the rift basins of eastern China. Notably, the relative fluctuations in lithospheric thickness in basins demonstrate significant disparities: basins rich in oil and gas often exhibit greater thickness fluctuations. Additionally, in the offshore basins of China, a conspicuous negative linear correlation is observed between the minimum lithospheric thickness and the relative fluctuation in lithospheric thickness. This study posits that deep-seated thermal upwelling results in lithospheric undulations and extensional thinning in oil and gas basins. Concurrently, sustained deep-seated heat influences sedimentary materials in basins, creating favorable conditions for oil and gas generation. The insights derived from this study contribute to a quantitative understanding of the intricate relationships between deep lithospheric structures and oil and gas basins. These findings provide valuable guidance for future oil and gas exploration in the studied areas.

Key words: China seas and adjacent areas, lithospheric thickness, oil and gas basins

Citation: Ma Jing, Wang Wanyin, Zeyen Hermann, Zhang Yimi, Li Zhongsheng, He Tao, Wang Dingding. 2024. Influence of lithospheric thickness distribution on oil and gas basins, China seas and adjacent areas. Acta Oceanologica Sinica, 43(4): 1–14, doi: 10.1007/s13131-024-2342-7

1 Introduction

In recent years, the interaction of the Earth's different spheres, especially how the dynamic processes of the solid Earth affect the evolution of the surface environment and the enrichment of energy resources, has become a major focus of interdisciplinary research. Therefore, an increasing number of scholars have proposed thinking about and studying "Earth system science" from a larger perspective in the future (Zhu et al., 2023). The China seas and adjacent areas are situated on the eastern part of the Eurasian continent, along the western coast of the Pacific Ocean. During the Mesozoic and Cenozoic, due to the intense dynamic and thermal activity involved in the process of rapid rifting and subduction of ancient crust in the western Pacific, the marginal seas in the western Pacific and the eastern margin of Asia and the rift basin system in eastern China have emerged (Li et al., 2018b). The lithospheric structure is complex and variable, and the tectonic activity in this region is dynamic. The presence of well-developed sedimentary basins offers large prospects for oil and gas exploration (Chen et al., 2019) (Fig. 1). While oil and gas resources are primarily concentrated within sedimentary basins, it is essential to recognize that the structure and evolution of the lithosphere fundamentally influence the accumulation of oil and gas resources. The distribution of oil and gas resources is intrinsically linked to deep-seated lithospheric characteristics (Jin et al., 2003). Therefore, understanding the lithospheric thickness characteristics in the region offshore of

Foundation item: This research is supported by the National Key Research and Development Plan project "Research on Comprehensive Processing and Interpretation Methods of Aeronautical Geophysical Data and Soft ware Development" under contract No. 2017YFC0602202.

*Corresponding author, E-mail: wwy7902@chd.edu.cn

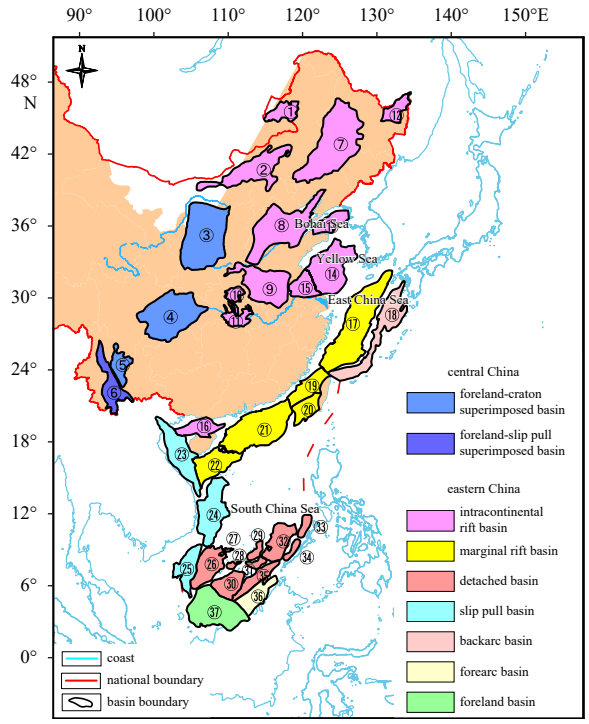

Fig. 1. Distribution of oil and gas basins in the China seas and adjacent areas (modified from Chen et al., 2019) ① Hailar Basin, ② Erlian, ③ Ordos Basin, ④ Sichuan Basin, ⑤ Chuxiong Basin, ⑥ Lanping-Simao Basin, ⑦ Songliao Basin, ⑧ Bohai Bay Basin, ⑨ South North China, ⑩ Nanxiang, ⑪ Jianghan Basin, ⑫ Sanjiang Basin, ⑬ North Yellow Sea, ⑭ Subei Basin, ⑮ South Yellow Sea, ⑯ Beibu Gulf, ⑰ East China Sea Shelf Basin, ⑱ Okinawa Trough Basin, ⑲ Taixi, ⑳ Taixinan, ㉑ Zhujiang River estuary, ㉒ Qiongdongnan Basin, ㉓ Yinggehai Basin, ㉔ Zhong Jiannan, ㉕ Wan'an, ㉖ Nanweixi, ㉗ Yongshu Basin, ㉘ Nanweidong, ㉙ Jiuzhang Basin, ㉚ Beikang Basin, ㉛ Andubei Basin, ㉜ Liyue, ㉝ North Palawan, ㉞ South Palawan, ㉟ Nansha Trough Basin, ㊱ Brunei-Sabah Basin, ㊲ Zengmu Basin,

China and adjacent areas is highly important for understanding the relationship between lithospheric structure and the distribution of oil and gas resources in oil-bearing basins.

The lithospheric thickness refers to the vertical distance from the Earth's surface to the lithosphere–asthenosphere boundary (LAB). Over the years, researchers have employed various methods to quantitatively estimate lithospheric thickness based on differences in lithospheric and asthenospheric properties. These methods include the following. (1) The geothermal lithospheric thickness has been calculated using heat flow data. (2) The seismic lithospheric thickness has been calculated using seismic wave propagation velocities and quality factors. (3) The electrical lithospheric thickness has been calculated using electromagnetic deep sounding data. The above three methods typically rely on single data sources, resulting in calculations with single attributes. Another approach involves integrating multiple data sources to calculate the lithospheric thickness, offering a more comprehensive geophysical basis for studying deep-seated lithosphere layers (Xu et al., 2016). In 1977, McKenzie and others proposed a method that combines heat, gravity, and lithosphere isostasy concepts for calculating lithospheric structure (McKenzie, 1977). In 1994, Hermann Zeyen et al. improved upon the calculation method (Zeyen and Fernàndez, 1994). In 2022, J. C. Afonso et al. studied three-dimensional lithospheric structure, temperature, density and composition by integrating various geophysical observation data (Afonso et al., 2022). At present, this method has been successfully applied in the study of various geological problems. The use of multiple high-resolution data sources to jointly calculate high-precision multiattribute lithospheric thickness is a new research trend.

With the continuous improvement of deep Earth geophysical data, research on the deep structure of oil and gas basins and their relationship with hydrocarbon accumulation has gradually evolved. The investigation of the geodynamic mechanisms of oil and gas basins has become a major trend in basin research. Thus, quantitative analysis of parameters reflecting deep processes is needed to understand the inherent relationship between basin evolution and lithospheric processes (He et al., 2004; Li, 2015). Previous studies have largely focused on qualitative analyses of the relationships between the deep lithosphere structure and oil and gas basins (Xu, 2003). However, only a few scholars have conducted semiquantitative analyses of the relationships between deep lithospheric structural parameters and the distributions of oil and gas resources in these basins (Li et al., 2018a; Zhang et al., 2023). Consequently, while some understanding of the relationship between lithospheric thickness characteristics and oil and gas basin distributions has been qualitatively established in previous research, identifying specific quantitative to semiquantitative patterns still requires further exploration during the investigation of the deep lithospheric structure in oil and gas basins.

In summary, prior research has extensively delved into lithospheric thickness calculations, and the inexorable shift toward computing high-precision multiattribute lithospheric thickness using diverse data sources is evident. However, there is a dearth of quantitative investigations into the nexus between lithospheric thickness characteristics and hydrocarbon abundance in oil and gas basins, and specific patterns warrant further exploration. Thus, grounded in the assumptions of local lithospheric isostasy and heat conduction principles, this study harnesses increasingly available data, including topographic, satellite gravity and geoid data, as well as information regarding sedimentary and crustal thickness and density, to calculate the lithospheric thickness for the China seas and adjacent areas. Utilizing the computed results, this paper employs statistical methods to scrutinize, for various types of oil and gas basins within the study area, the relationship between the minimum lithospheric thickness and hydrocarbon abundance. Ultimately, the paper delves into the mechanisms that underlie the correlation between lithospheric thickness and oil–gas richness in oil and gas basins. These findings provide valuable reference points for subsequent research on the quantitative relationships between deep lithospheric structures and oil and gas basins, aiding in the strategic selection of areas for future oil and gas exploration.

2 Lithospheric thickness calculation

2.1 *Data sources*

The digital elevation data and satellite gravity anomaly data used in the China seas and neighboring regions are from the latest version of the global satellite gravity database (V31.1) (https://topex.ucsd.edu/cgi-bin/get_data.cgi) (Sandwell et al., 2014). The grid resolution of the digital elevation data is 1′ × 1′ (Fig. 2). The satellite gravity anomaly data in the marine domain have a grid resolution of 1′ × 1′, with a total accuracy of up to 3.03 × 10^{-5} m/s², and locally achieve an accuracy of 1.8 × 10^{-5} m/s². In the terrestrial domain, the grid resolution is 5′ × 5′, with a total accuracy of 4.125 × 10^{-5} m/s² (Fig. 3). The geoid data used in the study area come from the EGM2008 Earth gravity data model

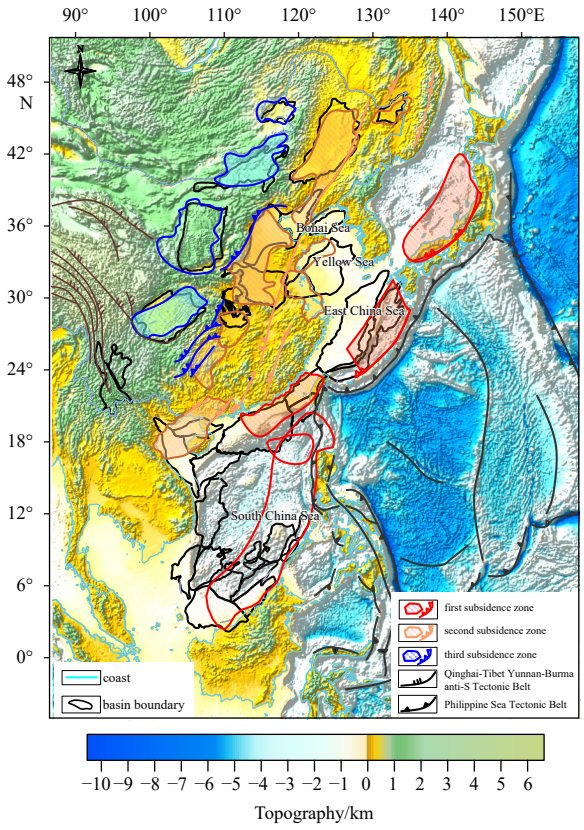

Fig. 2. Topographic elevation map of the China seas and adjacent areas.

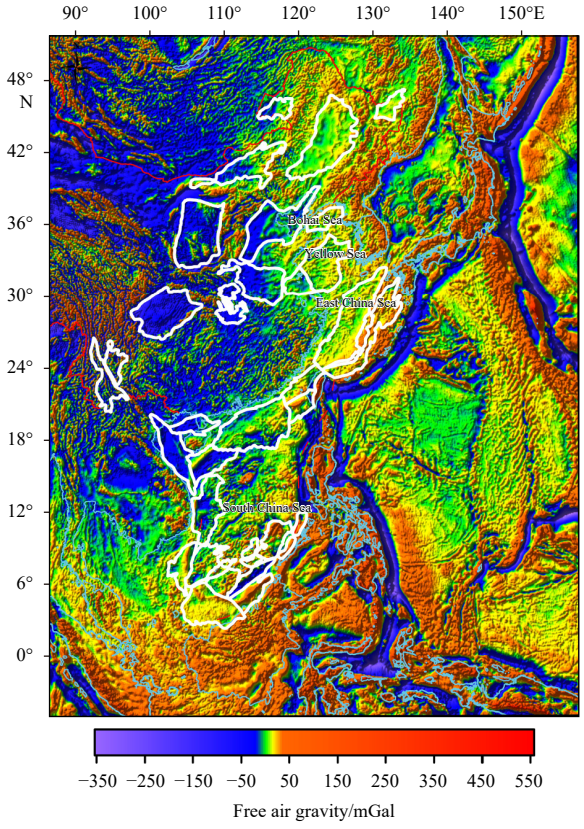

Fig. 3. Satellite gravity anomaly map of the China seas and adjacent areas.

(http://icgem.gfz-potsdam.de/tom_longtime). The grid resolution is 5′ × 5′, and the total accuracy can reach 15 cm (Pavlis et al., 2012). The total spherical harmonic coefficient of EGM2008 is 2 159, and this study focuses only on the lithosphere, so the deep influence of orders 1–11 is eliminated (Fig. 4). The marine sediment thickness data used in the study were obtained from Straume et al. (https://ngdc.noaa.gov/mgg/sedthick/) (Straume et al. 2019), with a grid resolution of 5′ × 5′. The terrestrial sediment thickness data and initial mantle density data are derived from the CRUST1.0 model, with a grid resolution of 1°×1° (https://igppweb.ucsd.edu/~gabi/crust1.html) (Laske et al., 2012) (Fig. 5). The variable sediment layer density, variable crustal density, and Moho depth data (Fig. 6) used in the study are from Zhang et al. (2023), with the root mean square deviation of the Moho depth to known constraint points being as low as 1.5 km.

2.2 *Method*

We subdivide the area into independent vertical columns of size 10×10 km. As shown in Figure 7, each column is split vertically into 4 layers (mention the layers). Under the assumption of local isostasy in the lithosphere, the depth of the LAB (Z_{LAB}) for each lithosphere column can be expressed by the following formula (Lachenbruch and Morgan, 1990; Fullea et al., 2007):

$$\begin{cases} Z_{\mathrm{LAB}} = \rho_a \dfrac{H + H_0 - \sum \left(\dfrac{\rho_a - \rho_i}{\rho_a} \right) d_i}{\rho_a - \rho_m} + Z_{\mathrm{Moho}}, \ H \geqslant 0, \\ Z_{\mathrm{LAB}} = \rho_a \dfrac{H \left(\dfrac{\rho_a - \rho_w}{\rho_a} \right) + H_0 - \sum \left(\dfrac{\rho_a - \rho_i}{\rho_a} \right) d_i}{\rho_a - \rho_m} + Z_{\mathrm{Moho}}, H < 0, \end{cases} \tag{1}$$

where H represents the topography of the column, ρ_a is the as-

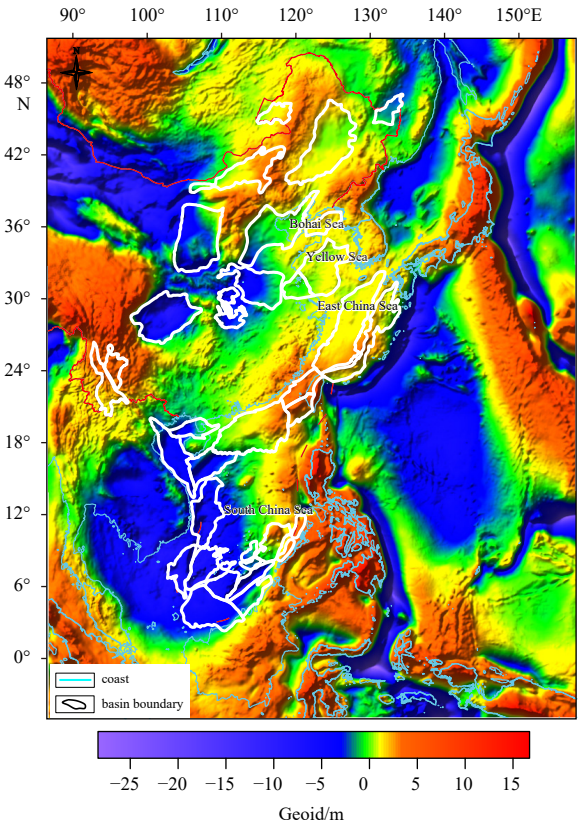

Fig. 4. Geoid map of the China seas and adjacent areas.

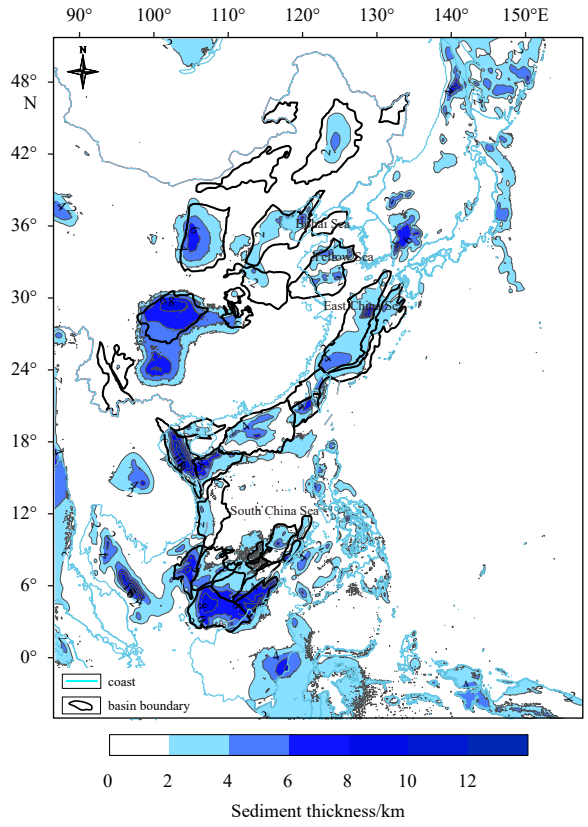

Fig. 5. Sediment thickness map of the China seas and adjacent areas.

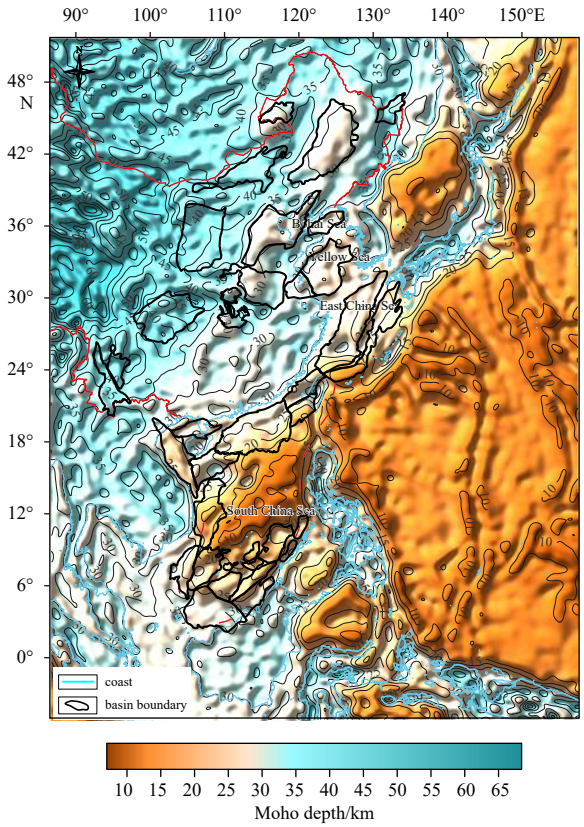

Fig. 6. Moho depth map of the China seas and adjacent areas.

thenosphere density, ρ_w is the seawater density, ρ_m is the average lithosphere mantle density, H_0 is an elevation calibration constant (Lachenbruch and Morgan, 1990), Z_{LAB} and Z_{Moho} are the depths of the lithosphere bottom interface and the Moho depth of the lithosphere column, and ρ_i and d_i are the density and thickness of crustal layer i, respectively. The lithospheric thickness is then calculated as follows:

$$L = Z_{\mathrm{LAB}} + H. \tag{2}$$

The formulas for calculating the topography and geoid of the lithospheric column are described previously, and (x, y, z) is the coordinates of the prism (Xu et al., 2016)

$$E = f\cdot\left(\frac{\rho_a-\rho_l}{\rho_a}L+E_0\right);\ f=\begin{cases}1, & H\geqslant 0\\ \dfrac{\rho_a}{\rho_a-\rho_w}, & H<0.\end{cases} \tag{3}$$

$$\Delta N = \frac{G\rho}{g}\left|\left|xy\ln(z+r)+yz\ln(x+r)+xz\ln(y+r)-P\right|_{x_1}^{x_2}\right|_{y_1}^{y_2}\Big|_{z_1}^{z_2}, \tag{4}$$

where

$$r=\sqrt{(x^2+y^2+z^2)},$$

$$P=\frac{z^2}{2}\arctan\left(\frac{xy}{zr}\right)+\frac{x^2}{2}\arctan\left(\frac{yz}{xr}\right)+\frac{y^2}{2}\arctan\left(\frac{xz}{yr}\right).$$

Under the assumptions of thermal equilibrium in the lithosphere and the absence of lateral heat transfer between lithosphere columns, with surface and LAB temperatures of T_s = 5℃ and T_a = 1 330℃, respectively, the temperature T_{Moho} at the crust–mantle boundary can be expressed as follows (Fullea et al., 2007):

$$T_{\mathrm{Moho}}=\frac{(Z_{\mathrm{LAB}}-Z_{\mathrm{Moho}})\left\{k_cT_s+A_sa_r^2\left[1-\exp\left(-\dfrac{Z_{\mathrm{Moho}}+H}{a_r}\right)\right]\right\}+k_mT_a(Z_{\mathrm{Moho}}+H)}{Z_{\mathrm{Moho}}(k_m-k_c)+Z_{\mathrm{LAB}}k_c+Hk_m}, \tag{5}$$

where k_c and k_m are the average crustal and mantle thermal conductivities, respectively. As the surface radioactive heat production, a_r is a parameter describing the exponential decay of heat production with depth (Table 1). The lithospheric mantle density has a linear relationship with temperature, and the average mantle density of the lithospheric column unit ρ_m is expressed as follows (Parsons and Sclater, 1977):

$$\rho_m=\rho_a\left[1+\frac{\alpha}{2}(T_a-T_{\mathrm{Moho}})\right]. \tag{6}$$

Based on the above formula, the lithospheric thickness calculation scheme is given. First, the structure of the initial lithosphere model is established according to the collected prior information. Second, the iterative process of determining the bottom interface depth of the lithosphere Z_{LAB} is established. Based on the initial lithospheric model data, Eqs (3), (4), (5) and (6) are used to obtain the first calculated values $E^{(1)}$, $\Delta N^{(1)}$, $T^{(1)}_{\mathrm{Moha}}$, and $\bar{\rho}_m^{(1)}$, respectively, and the calculated geoid and topography are compared with the measured geoid and topography. Third, we

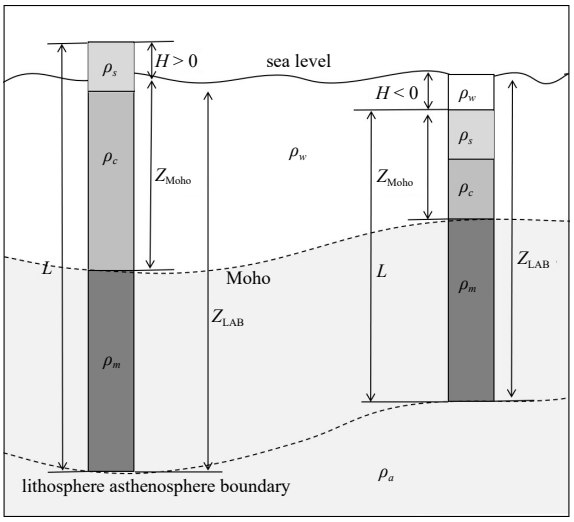

Fig. 7. Schematic diagram of lithospheric local isostasy theory (modified from Fullea et al., 2007).

determine whether the iteration accuracy is satisfactory. If these conditions are met, the depth of the bottom interface of the lithosphere is obtained. If the conditions are not met, the next depth of the bottom interface of the lithosphere is calculated according to the iterative process of the second step until the conditions are met and L is obtained (Figs 8 and 10).

2.3 *Results*

Figure 8 is a lithospheric thickness map for the study area that shows the lithospheric thickness in the region ranges from 40 km to 170 km. Xu et al. used the calculation method in this study to calculate the LAB depth in the North China Craton in 2016. After comparison, the calculation results in this paper are consistent with its shape, and the results are similar (Xu et al., 2016). The lithospheric thickness is thick in the mainland region and thin in the ocean, thus exhibiting clear east-west zonation, which reflects the interaction of the three major tectonic plates in the deep lithosphere. The primary trend of lithospheric thickness in the entire region is oriented in the NE-NNE direction, and the lithospheric thickness primarily ranges from 80 km and 100 km, forming distinct lithospheric thickness gradient zones.

In continental areas, the lithospheric thickness ranges from 80 km to 165 km, and the LAB depth has an obvious positive correlation with the Moho depth and a weaker positive correlation with the topography (Fig. 9). The thickest region is in the Qinghai-Tibet Plateau, which represents a region with significant lithospheric thickness variation is the result of the final closure of the long-developed Tethys Ocean in the late Paleozoic and the collision of Gondwana and Asia (Li et al., 2018a). The lithospheric thickness decreases markedly from west to east. From the island to the trench, the lithospheric thickness thickens sharply from 80 km to 100 km, and the gradient changes greatly, presenting a strip-like lithospheric thickening zone along the trench subduction zone. In oceanic regions, the lithosphere is thinner, ranging from 70 km to 110 km, and the changes in lithospheric thickness are gradual.

In continental regions in central and eastern China, the lithospheric thickness exhibits a stepwise decrease from west to east, with the lithosphere base continually rising. In the Bohai and Yellow Seas, the lithospheric thickness ranges from 70 km to 85 km. On the East China Sea shelf, the lithospheric thickness ranges

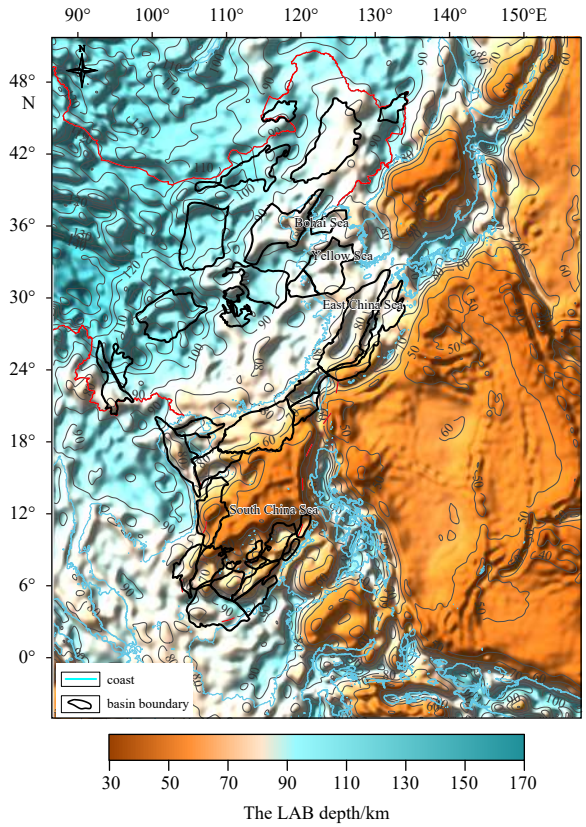

Fig. 8. Lithospheric thickness map of the China seas and adjacent areas.

from 70 km to 85 km, and the lithosphere thins toward the southeast. In continental shelf areas, the lithospheric thickness remains relatively stable. It decreases slightly from 85 km in the continental crust area to 75 km in the southeast, with noticeable uplift of the LAB in the center of the East China Sea Shelf Basin center, resulting in a thinner lithosphere than in the surrounding areas. In the Okinawa Trough area, there is a same trend from north to south. In the southern part of the trough, the lithosphere is thinnest, at approximately 70 km. In the South China Sea, the lithospheric thickness ranges from 50 km to 70 km, exhibiting complex undulations in the lithosphere base. There are significant variations in lithospheric thickness. In the continental crust regions located in the northern, western, and southern margins of the South China Sea, the lithospheric thickness ranges from 65 km to 70 km, gradually thinning from the continental margin to the basin, with minor uplift of the lithosphere base. In the transitional crust regions in the northern, western, and southern continental slopes of the South China Sea, the lithospheric thickness ranges from 55 km to 65 km, with significant thinning and dramatic uplift of the lithosphere base toward the basin, forming distinct gradient zones. In the oceanic crust regions of the basin, the lithospheric thickness changes are relatively gentle, ranging from 50 km to 55 km. The southwestern and northwestern subbasins exhibit slightly thinner lithosphere than the central basin.

In the Sea of Japan, the lithospheric thickness ranges from 43 km to 70 km. Moving from the central basin toward the edges, the lithospheric thickness gradually increases. To the west, the lithospheric thickness rapidly increases to 70 km, extending to the Korean Peninsula, whereas to the east, it thickens significantly toward the Japanese islands. The Japan Sea Basin features oceanic crust, with lithospheric thicknesses ranging from 43 km

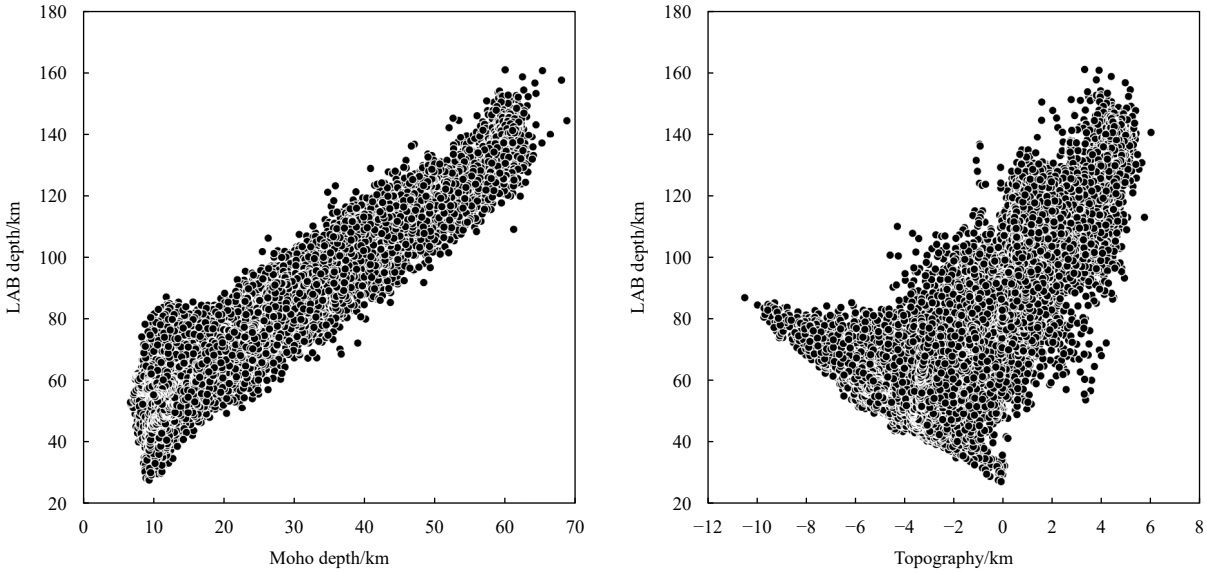

Fig. 9. Relationships between the LAB depth and the Moho and topography depth.

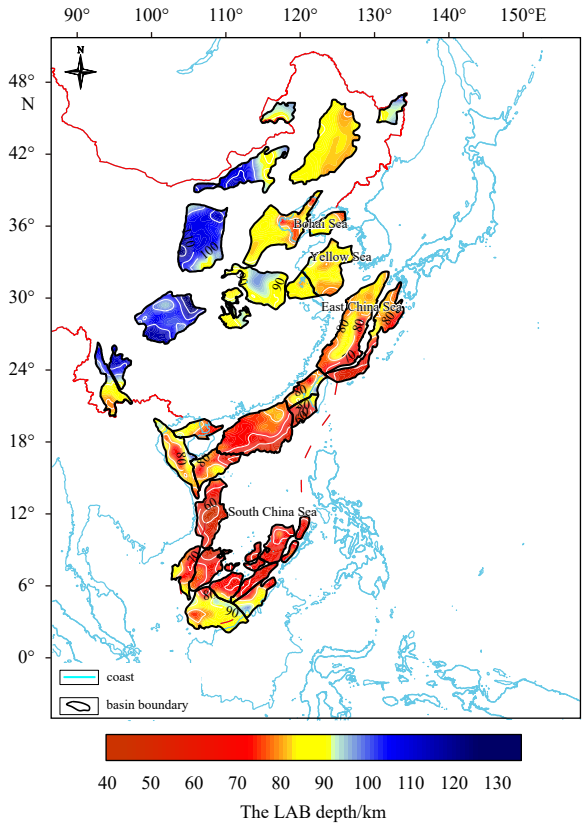

Fig. 10. Lithospheric thickness map of oil and gas basins in the China seas and adjacent areas.

to 50 km and thinning in the eastern part. The Tsushima and Yamato basins have thin lithosphere with lithospheric thicknesses ranging from 50 km to 55 km. The Yamato Ridge has continental crust with lithospheric thicknesses ranging from 55 km to 60 km. The lithospheric thickness of the Japanese archipelago is greater than 60 km and exhibits significant variation, forming a gradient zone.

In the West Philippine Sea, which includes the West Philippine Basin, Palawan Trough, and Sulu Sea Basin, the lithospheric thickness ranges from 38 km to 68 km, with an uplifted lithospheric base. The undulations in the lithospheric thickness base gradually vary. Except for a small central area in the West Philippine Basin, the lithospheric thickness is generally less than 60 km. In the eastern part of the Sulu Sea Basin, the lithospheric thickness decreases to approximately 40 km. In the Caroline Sea, the lithospheric thickness ranges from 40 km to 60 km, indicating a thinned lithospheric thickness with gradual fluctuations.

Table 1. Calculation parameters

Parameters	Property of matter	Parameter value
ρ_a	Asthenosphere density (g/cm^3)	3.2
ρ_w	Sea water density (g/cm^3)	1.03
H_0	Elevation calibration constant (m)	140
α	Coefficient of mantle thermal expansion (10^{-5} K^{-1})	3.5
T_s	Surface temperature (℃)	5
T_a	Lithosphere-asthenosphere boundary temperature (℃)	1 330
A_s	Heat yield of surface rocks (10^{-6} W/m^3)	2.5
a_r	The constant factor of exponential distribution of crustal rock heat yield (10^3)	15
k_c	Crustal heat conductivity (W/(K·m))	2.5
k_m	Mantle heat conductivity (W/(K·m))	3.3

3 Relationships between lithospheric thickness and oil and gas basins

Historically, oil and gas exploration has focused on the study of the essential factors contributing to the formation of hydrocarbon reservoirs, such as source rocks, reservoirs, seals, traps, and the migration and preservation of oil and gas. Research on oil and gas basins has primarily centered on reconstructing the burial history and tectonic deformation history of sedimentary cover layers (Jin et al., 2003). However, little attention has been given to the deep structural characteristics of these basins and their correlation with hydrocarbon potential. Considering the profound influence of deep lithospheric structural evolution on the formation and evolution of oil and gas basins (Li, 2015), there is a cru-

cial need to explore the relationship between lithospheric thickness and the distribution of oil and gas resources. By utilizing lithospheric thickness parameters, this study aims to enhance the efficiency of oil and gas exploration.

Figure 10 shows the lithospheric thickness in the oil and gas basins of the study area. The lithospheric thickness in these basins ranges from 48 km to 135 km. In China's continental crust basins, the lithospheric thickness is generally greater (exceeding 85 km) than that in oceanic basins (less 85 km). Nearshore basins in China are situated in the transition zone between continental margin crust and oceanic crust, resulting in a gradual reduction in lithospheric thickness from the northwest to southeast. China's oceanic crust basins feature thin lithosphere, typically less than 75 km thick. Overall, the oil and gas basins in the study area exhibit a pattern of thinning lithosphere from northwest to southeast, which contributes to a diverse distribution of oil and gas resources. This variation in lithospheric thickness within the oil and gas basins gives rise to a range of oil and gas distribution patterns. Li Siguang proposed that the formation and evolution of three subsidence zones controlled the development of oil and gas basins (Kang et al., 2019) (Fig. 1). The lithospheric thickness distribution in this study correlates well with these three subsidence zones. The first subsidence zone, where basins have relatively thin lithospheric thicknesses (48–85 km), is located mainly within areas of thinning oceanic lithosphere. This area includes the basins in the South China Sea, East China Sea shelf, and Yellow Sea. The second subsidence zone, featuring basins with lithospheric thicknesses transitioning from thick to thin (85–95 km), corresponds to regions in the transition zone of lithospheric thickness in eastern and central China. This area includes the Songliao Basin, Bohai Bay Basin, North China Basin, Nanxiang Basin, Jianghan Basin, Sanjiang Basin, and northern part of the Beibu Gulf Basin. The third subsidence zone, with basins displaying relatively thick lithosphere (95–135 km), is situated within areas with thicker continental crust. This zone includes the Hailar Basin, Erlian Basin, Ordos Basin, Sichuan Basin, Chuxiong Basin, and Lanping-Simao Basin (Kang et al. 2019). The variation in lithospheric thickness within the oil and gas basins reflects the distribution of the New China Orogenic System, validating the scientific significance of studying the three subsidence zones that control basin development and oil and gas resources.

Table 2 presents statistical data on geological resource quantities in oil and gas basins in the research area, along with lithospheric thickness parameters (Zheng et al., 2019; Xie and Gao, 2020). Notably, the oil and gas basins with relatively high total hydrocarbon equivalents include Bohai Bay, Zengmu, Ordos, Songliao, Sichuan, the Zhujiang River estuary, Zhong Jiannan, Qiongdongnan, the East China Sea shelf, Wan'an, Brunei-Shaba, Yinggehai, and the Beibu Gulf basins. Using data-driven methodologies and employing principles of mathematical statistics, this paper explores the semiquantitative relationship between lithospheric thickness and hydrocarbon potential in oil and gas basins. First, considering the different types of basins, we statistically analyzed two lithospheric thickness parameters: the minimum lithospheric thickness and the relative variation in lithospheric thickness. Subsequently, by integrating known total geological oil-equivalent resources, we analyzed the semiquantitative relationship between these lithospheric thickness parameters and the total geological oil-equivalent resources in oil and gas basins (Figs 11, 12 and 13). This study provides valuable insights into the quantitative and semiquantitative relationships between the deep lithosphere structure and hydrocarbon potential in basins, offering a reference for future research on the quantitative and qualitative relationships in oil and gas exploration zones.

(1) The lithospheric thickness obviously differs among the basins. It is thicker in the superimposed basins in central China and thinner in the rift basins in eastern China.

Figure 11 shows a statistical analysis of the minimum lithospheric thickness in the oil and gas basins in the research area. The minimum lithospheric thickness (L_{min}) represents the thinnest part of the lithosphere in the studied oil and gas basins. The chart indicates that the superimposed basins in central China exhibit a large range in lithospheric thickness, fluctuating between 76 km and 91 km. The Sichuan Basin, Ordos Basin, Chuxiong Basin, and Lanping-Simao Basin are Mesozoic–Cenozoic foreland–craton superimposed basins. These basins developed as cratonic basins in the Mesozoic and foreland basins in the Cenozoic (He et al., 2004), with lithospheric thicknesses exceeding 85 km. The Sichuan Basin is located on the Sichuan block, a portion of the Yangtze block, with a thickness of up to 91 km. The Ordos Basin, situated on the Ordos block (part of the North China block), has a thickness of 88 km. They are located north and south of the Qinling orogenic belt. The Chuxiong Basin, located in the southwest of the Sichuan block, has a thin lithospheric thickness of 85 km. The Lanping-Simao Basin, a foreland-extension overlapping basin, is relatively thin, with a thickness of 76 km. These basins are situated on the eastern and western sides of the Ailao Shan orogenic belt. Overall, a thicker lithosphere in the central superimposed basin in China corresponds to better oil and gas characteristics. The Sichuan Basin and Ordos Basin have thicker lithosphere and more abundant oil and gas resources than the Chuxiong Basin and Lanping-Simao Basin. In particular, the Sichuan Basin is still in the early stages of exploration, with significant potential for future oil and gas resource development (Dai et al., 2021).

The intracontinental rift basins in the research area include intraplate fault basins and intraplate multicyclic fault basins, which have more variable lithospheric thicknesses than the central superimposed basins (Li, 1982). The intraplate fault basins have thicker lithosphere than the intraplate multicyclic fault basins. For example, the Songliao Basin, which has abundant oil and gas resources and is located on the Songnen block, has the thinnest lithosphere (78 km), while the Erlian, Sanjiang, and Hailaer basins have larger lithospheric thicknesses, all exceeding 85 km.

Continental marginal rift basins, situated on the Yangtze block of the Yangtze-Jingxi block, exhibit diverse lithospheric thicknesses ranging from 47 km to 72 km. Among them, the Zhujiang River estuary, Qiongdongnan Basin, Taixinan, and East China Sea Shelf Basin have relatively thin lithospheric thicknesses, all of which are less than 60 km. The Zhujiang River estuary Basin has the thinnest lithospheric thickness of 47 km, and it also has the highest total oil resource equivalents.

The slip pull basins in the research area are oil and gas basins that developed in the transitional zone between the Indochina block and the South China block (Zhang et al., 2015). The lithospheric thickness varies significantly, ranging from 43 km to 70 km. For instance, the Zhong Jiannan Basin has the thinnest lithosphere at 43 km and relatively higher total oil resource equivalents.

The backarc basins, located on the South China Sea block, are Cenozoic basins with thin lithospheric thicknesses ranging from 48 km to 67 km. The Yongshu Basin has the thinnest lithosphere at 48 km. Additionally, the Zengmu Basin and Brunei-Shaba Basin, which developed on the thinned crust of the early passive continental margin of the Borneo block, have relatively thick

Table 2. Statistical table of geological resources (Zheng et al., 2019; Xie and Gao, 2020) and lithospheric thickness parameters in the China seas and adjacent oil and gas basins

Basin type	Basin name	Basin area L_s/ km^2	Oil geological resources/ 10^8t	Gas geological resources/ 10^8m^3	Total oil resource equivalent/ 10^8t	Oil abundance/ (10^5t·km^2)	Minimum lithospheric thickness L_{min}/km	Relative fluctuation difference $\Delta L/10^2$km	Average sedimentary thickness L_{sed}/km	Average heat flow Q(mW·m^{-2})
Superimposed basins	Chuxiong	43 200	–	–	–	–	84	34	0.8	74
	Lanping-Simao	75 850	–	–	–	–	76	34	0.3	63
	Ordos	237 025	116.5	23 636.3	135.3	57.1	89	29	3.5	66
	Sichuan	198 550	–	124 655.8	99.3	50.0	91	29	6.4	55
Continental rift basin	Songliao	264 975	111.4	26 734.9	132.7	50.1	75	23	1.7	64
	Hailar	43 500	10.1	841.8	10.8	24.8	88	9	0.5	57
	Erlian	139 200	13.4	–	13.4	9.6	88	26	0.2	71
	Sanjiang	39 425	–	–	–	–	86	17	0.2	48
	South North China	144 175	–	–	–	–	82	16	1.3	60
	Bohai Bay	20 2000	325.3	236 074.1	513.4	254.1	72	23	2.3	61
	Beibu Gulf	51 950	21.2	–	21.2	40.8	74	22	2.1	62
	Nanxiang	18 950	5.2	400.0	5.5	28.9	82	14	1.4	50
	South Yellow Sea	49 000	7.3	1 847.0	8.8	18.0	80	11	0.7	76
	Jianghan	37 125	5.2	–	5.2	13.9	83	15	2.5	50
	North Yellow Sea	44 300	4.2	–	4.2	9.6	76	20	1.0	51
	Subei	157 675	6.2	600.0	6.7	4.2	78	17	2.5	67
Continental margin rift basin	Qiongdongnan	89 025	14.9	51 607.0	56.0	62.9	55	43	4.2	80
	Zhujiang River estuary	249 300	74.3	29 958.0	98.2	39.4	47	43	2.4	66
	East China Sea Shelf	247 600	2.7	60 479.0	50.9	20.6	60	33	3.1	78
	Tai Xinan	47 650	1.2	805.0	1.9	3.9	50	45	3.6	69
	Tai Xi	64 800	0.6	1 248.0	1.6	2.5	72	28	2.1	65
Strike-slip and extensional basin	Wan'an	66 225	23.1	27 463.0	45.0	68.0	63	31	5.2	67
	Zhongjiannan	127 175	33.7	51 980.0	75.1	59.1	43	47	1.9	94
	Yinggehai	117 950	–	44 209.0	35.2	29.9	70	31	5.7	81
Detached continental block basin	Beikang	56 350	8.9	14 855.0	20.7	36.7	64	30	4.2	64
	Liyue	70 300	6.1	16 644.0	19.4	27.6	54	33	2.5	42
	Nanwei Dong	5 875	0.9	897.0	1.6	27.1	65	15	2.7	66
	Nanwei Xi	80 225	8.8	13 382.0	19.4	24.2	48	41	3.0	68
	Yongshu	2 275	0.3	294.0	0.5	22.9	54	14	2.3	98
	North Palawan	17 275	1.4	2 178.0	3.1	18.0	53	26	2.3	67
	South Palawan	13 150	0.9	1 471.0	2.1	15.9	67	15	3.8	40
	Nansha Trough	46 275	3.2	3 271.0	5.8	12.6	53	41	3.1	53
	Andubei	11 950	0.7	708.0	1.3	10.5	59	20	2.0	59
	Jiuzhang	14 525	0.8	825.0	1.5	10.1	56	23	2.0	35
Backarc basin	Okinawa trough	137 925	2.2	5 368.0	6.5	4.7	54	41.2	2.2	98
Forearc basin	Brunei-Sabah	63 725	31.7	15 274.0	43.9	68.8	65	33.4	7.5	49
Foreland Basin	Zengmu	161 250	29.6	165 966.0	161.8	100.3	64	32.9	6.0	70

Note: "–" indicates no data.

lithosphere (approximately 65 km). In summary, rift basins in eastern China exhibit better oil and gas characteristics when the lithospheric thickness is thinner. This pattern has been observed in basins such as the Taixi, South Palawan, Nanweidong, and Beikang, all of which show good potential for oil and gas exploration.

In the rift basins in eastern China, the potential source rock is considered an internal factor for oil and gas formation, while heat is an external factor (Zhang et al., 2010); the coupling of these two factors controls the generation of oil and gas in the basin, the scale of hydrocarbon generation, and the regional distribution patterns of petroleum or natural gas. Hence, in rift basins with thinner lithospheric thicknesses, the uplift of the upper mantle is more intense, and proximity to the asthenosphere results in a more intense heat source. We consider this relationship to reflect the cocontrolling effect of heat and source.

In the central superimposed basins in China, which formed within stable continental blocks with weak magmatic activity in

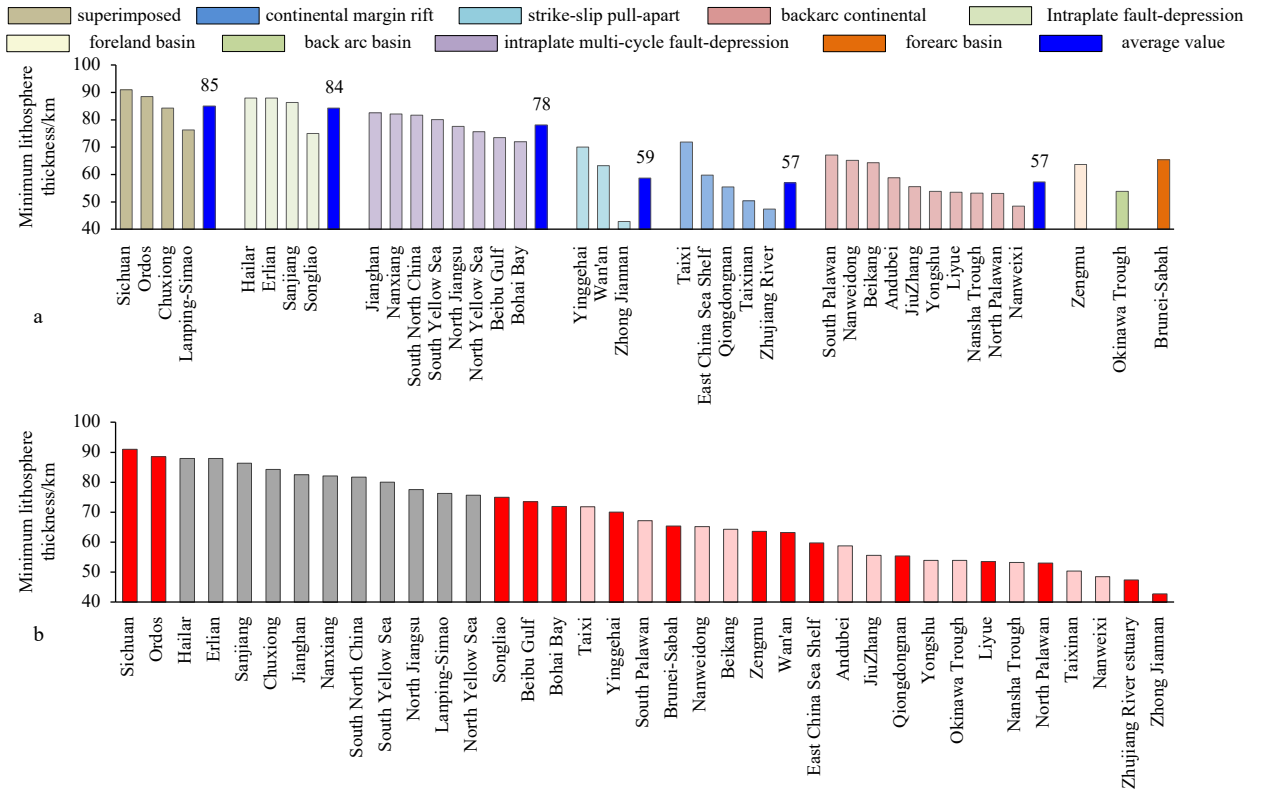

Fig. 11. Statistical chart of the minimum lithospheric thickness in the China seas and adjacent oil and gas basins a. Statistics according to the type of oil and gas basin; b. statistics according to the minimum thickness of the lithosphere in the oil and gas basin.

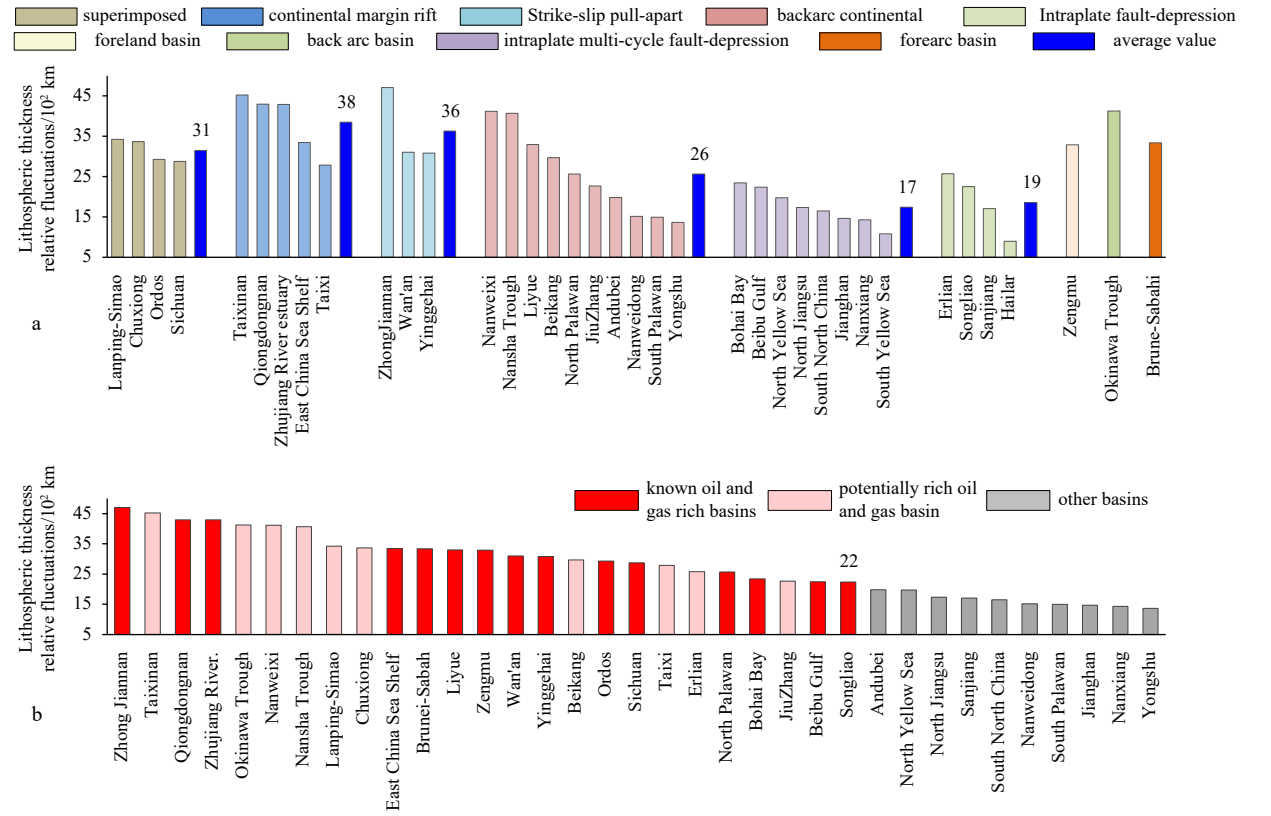

Fig. 12. Statistical chart of relative lithospheric thickness fluctuation in the China seas and adjacent oil and gas basins a. Statistics according to the type of oil and gas basin; b. statistics according to the relative fluctuation in lithospheric thickness in oil and gas basins.

the Mesozoic and Cenozoic, the geological background has been relatively stable. The deep thermal conditions are insufficient to cause lithospheric stretching. After prolonged heat dissipation and sedimentary loading, the heat flow is relatively low in these basins. Therefore, when the lithospheric thickness is greater, the lithosphere is more stable, deep magmatic activity is weaker, and the impact on the oil and gas reservoirs is weaker, ensuring more stable accumulation and trapping of oil and gas (Wang et al., 1998; Jin et al., 2003). We consider this relationship to reflect the controlling effect of a stable geological background.

In summary, the lithospheric thicknesses in oil and gas basins of different types exhibit distinct segmentation, reflecting the diversity in deep structural features among different types of oil and gas basins. In the central superimposed basin in China, when the lithospheric thickness is greater, the oil and gas characteristics are better, and the distribution patterns of oil and gas, represented by the minimum lithospheric thickness and total oil resource equivalents, follow a “thick-rich, thin-poor” pattern. In the eastern rift basins of China, when the lithospheric thickness is thinner, the oil and gas characteristics are better, and the distribution pattern follows a “thin-rich, thick-poor” pattern.

(2) The variations in lithospheric thickness in basins exhibit significant differences, with richer oil and gas basins often exhibiting larger relative fluctuations in lithospheric thickness.

There is a considerable difference in lithospheric thickness within oil and gas basins in the research area. The lateral variation in lithospheric thickness within basins reflects the heterogeneity and varying degrees of changes and deformation in the lithosphere (Li et al., 2018b). This study calculates the relative lithospheric thickness fluctuation (ΔL) in different types of oil and gas basins in the research area using Formula (7), which reflects the degree of variation in lithospheric thickness within a basin. A larger ΔL indicates greater changes in lithospheric thickness in an oil and gas basin, with $L_{\max}$ and $L_{\min}$ representing the maximum and minimum lithospheric thickness values in a given basin.

$$\Delta L = (L_{\max} - L_{\min})/L_{\max}. \tag{7}$$

The statistical analysis results shown in Table 2 (Fig. 12) reveal distinct differences among oil and gas basins of different types in the research area. Moreover, there is a certain relationship between ΔL and the abundance of oil and gas in these basins. Figure 12a shows that superimposed basins, margin rift basins, and transtensional basins generally have larger ΔL values, ranging from 30 km to 47 km. The separated block basins exhibit a wider range of variation, from 14 km to 41 km. Intraplate rift basins (intraplate multicyclic fault basins and intraplate fault basins) generally have smaller ΔL values, ranging from 10 km to 23 km. Notably, basins such as the Bohai Bay, Beibu Gulf, and

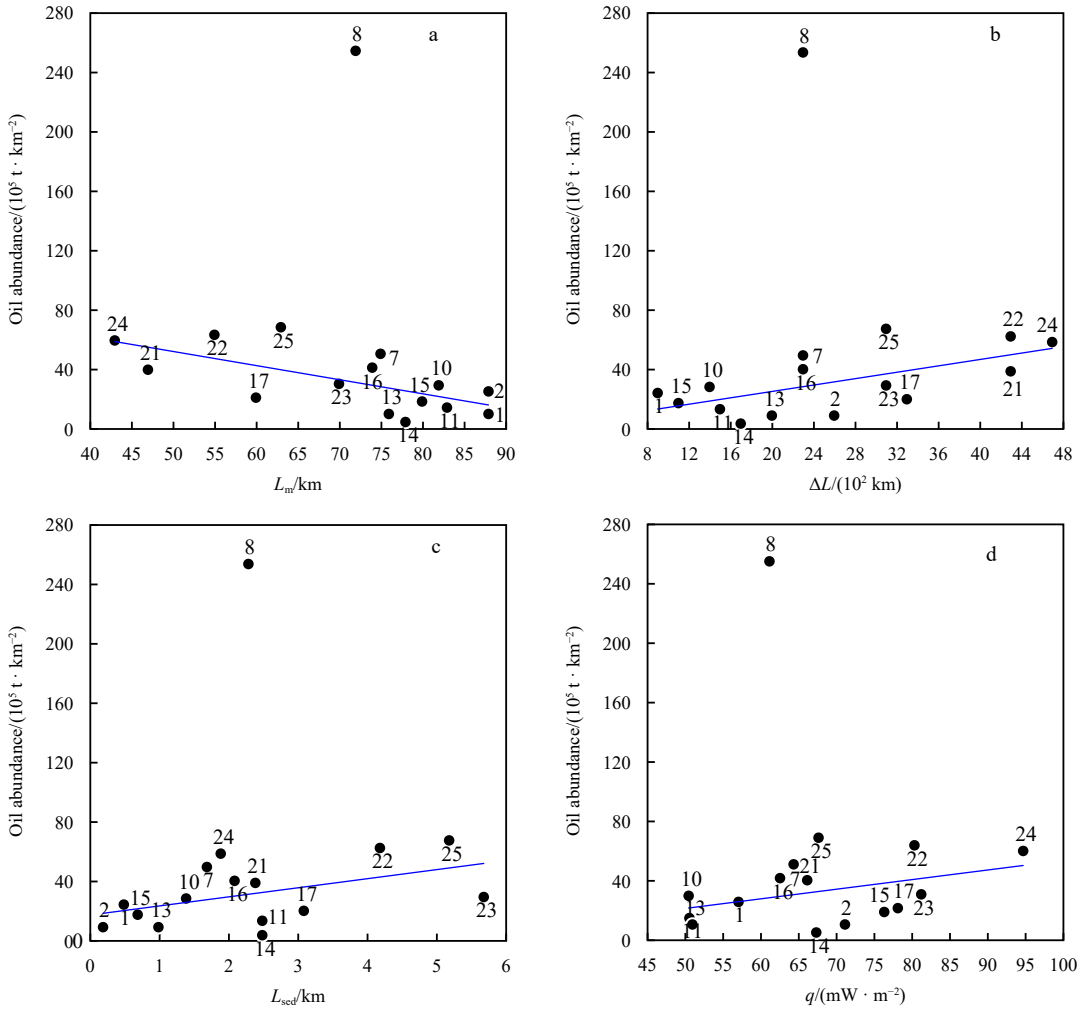

Fig. 13

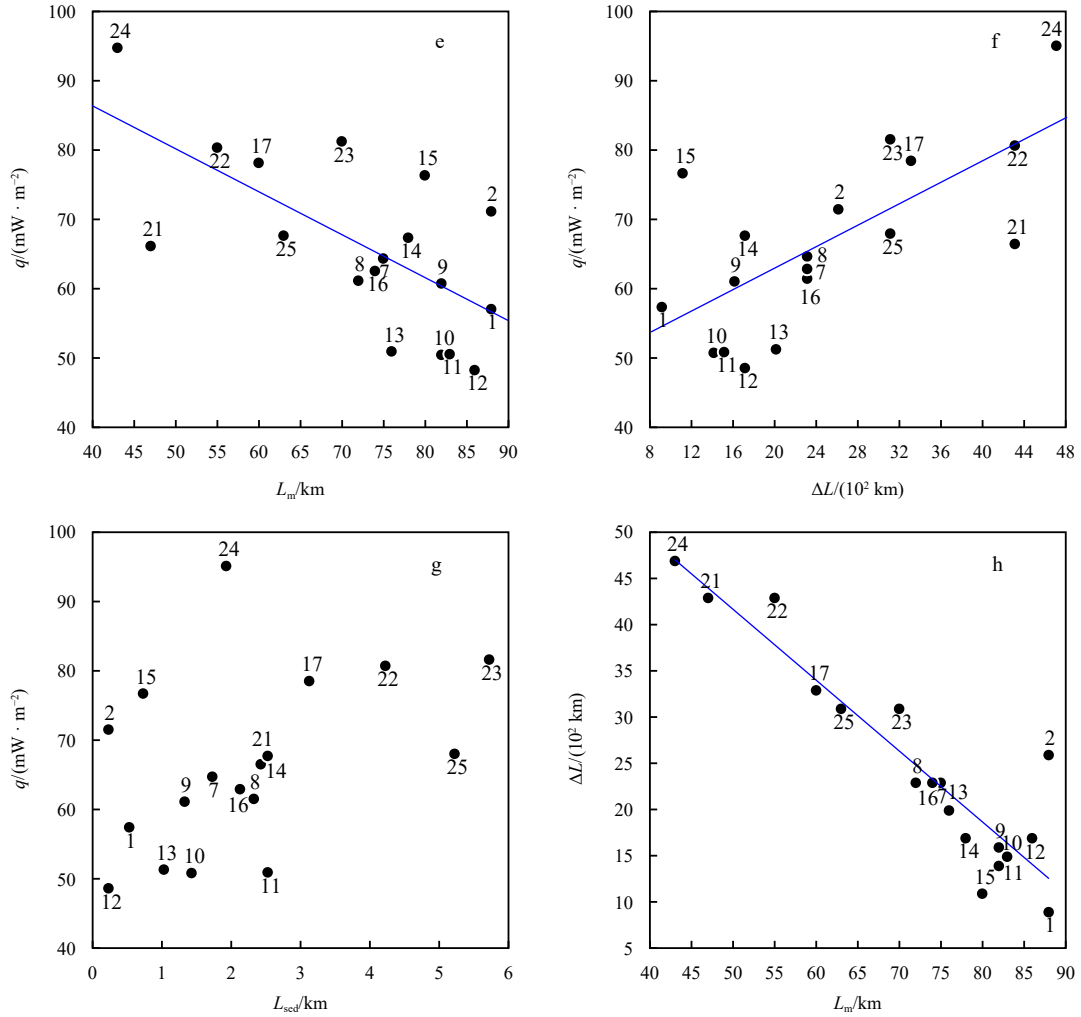

Fig. 13. Plots of lithospheric thickness in the China seas and adjacent oil and gas basins a. Minimum lithospheric thickness and oil abundance; b. relative lithospheric thickness fluctuation and oil abundance; c. sedimentary layer thickness and oil abundance; d. heat flow value and oil abundance; e. lithospheric minimum value and heat flow value; f. relative lithospheric thickness fluctuation and heat flow value; g. sedimentary layer thickness and heat flow value; h. lithospheric thickness minimum value and relative lithospheric thickness fluctuation difference. Note: 8 Bohai Bay Basin; 7 Songliao Basin; 9 South North China Basin; 12 Sanjiang Basin; 21 Zhujiang River estuary Basin; 22 Qiongdongnan Basin; 17 East China Sea Shelf Basin; 16 Beibu Gulf Basin; 2 Erlian Basin; 1 Hailar Basin; 15 South Yellow Sea Basin; 14 Subei Basin; 10 Nanxiang Basin; 11 Jianghan Basin; 13 North Yellow Sea Basin; 25 Wan'an Basin; 24 Zhong Jiannan Basin; 23 Yinggehai Basin

Songliao Basins have larger values, while others have smaller values. Figure 12b illustrates that basins with higher total oil resource equivalents generally have larger ΔL values, ranging from 22 km to 47 km. Among the known oil-rich basins, the Songliao Basin has the lowest value at 22 km, while the values of the other basins are all greater than 22 km. These findings suggest that basins such as Chuxiong, Lanping-Simao, Taixinan, the Okinawa Trough, the Nansha Trough, Nanweixi, Taixi, and Beikang have better oil and gas characteristics. The deep processes in the lithosphere are crucial controlling factors for basin development and evolution. Different types of basins undergo changes in lithospheric thickness during sedimentation. The structural evolution of oil and gas basins in the research area exhibits segmented and differentiated characteristics (Zhu et al., 2015). Under different tectonic conditions, the relative fluctuations in lithospheric thickness in oil and gas basins exhibit obvious segmentation and differences. The relative lithospheric thickness fluctuation represents the difference between the maximum and minimum lithospheric thicknesses in an oil and gas basin, visually reflecting the magnitude of the relative fluctuations in lithospheric thickness within the studied basins. A greater relative fluctuation suggests a greater degree of later-stage modification to the lithospheric thickness in an oil and gas basin, indicating the intensity of upwelling in the upper mantle or tectonic activity to some extent. If tectonic activity does not damage the oil and gas reservoirs in the basin, a larger relative fluctuation implies a greater amount of heat provided by the upper mantle. Additionally, these findings indicate that the basin has more space to store oil, providing favorable conditions for hydrocarbon generation.

In summary, the relative fluctuations in lithospheric thickness in oil and gas basins in the research area exhibit obvious segmentation and differences. The magnitude of the relative fluctuations in lithospheric thickness within oil and gas basins is a key factor influencing the oil and gas characteristics of these basins. A larger relative lithospheric thickness fluctuation in an oil and gas basin is one of the indicators of abundant oil and gas

in the basin.

(3) In the offshore basins of China, there is an obvious negative linear correlation between the minimum lithospheric thickness and the relative lithospheric thickness fluctuation.

As described above, both the lithospheric thickness and the variability in the lithospheric thickness in oil- and gas-bearing basins are crucial factors affecting the abundance of hydrocarbons. However, the precise semiquantitative nature of these relationships has yet to be determined. Notably, known oil-rich basins in the offshore areas of China include the Bohai Bay, Zhujiang River estuary, Zhong Jiannan, Qiongdongnan, East China Sea shelf, Wan'an, Brunei-Sabah, Yinggehai, and Beibu Gulf. Presently, further exploration of the semiquantitative relationships among various parameters in these oil- and gas-bearing basins offshore of China has been performed here. Figure 13 illustrates that Bohai Bay is a superrich oil and gas basin that is distinct from the others. In these basins, there is an approximate negative correlation between oil abundance and minimum lithospheric thickness, while oil abundance displays approximately positive correlations with lithospheric thickness variability, sediment layer thickness, and heat flow. This indicates that thicker sediment layers, higher heat flow values, and thinner lithospheric thickness are favorable conditions for hydrocarbon formation in these basins. Simultaneously, there is an approximately negative correlation between the relative variability in lithospheric thickness and the minimum lithospheric thickness in the offshore basins of China. From the statistical results, it is observed that while the maximum thicknesses in oil-bearing basins are relatively similar, the differences in the minimum thickness are significant, thus leading to large relative fluctuations in these basins. Consequently, a thinner lithospheric thickness in a basin corresponds to a greater relative fluctuation.

In summary, during the evolution of oil- and gas-bearing basins, the thinness of the lithosphere, variability in lithospheric thickness, sediment layer thickness, and heat flow all play crucial roles in determining the hydrocarbon abundance. Hence, a thinner lithosphere, greater lithospheric relative fluctuation, thicker sediment layers, and greater heat flow are indicative of oil- and gas-rich basins.

4 Discussion

Oil and gas result from the gradual transformation of organic matter deposited in sedimentary basins and buried to a certain depth under specific conditions, during which various biological processes occur (Tian and Shi, 2002). The presence and distribution patterns of oil and gas in sedimentary basins are closely related to the development and evolution of the basins. The formation of sedimentary basins is intricately linked to the internal structural architecture and thermal convection of the Earth. Therefore, studying the relationship between the structural properties of the lithosphere and basin formation is essential. The distribution of lithospheric thickness reflects the structure and properties of the lithosphere. Lithospheric layers of different thicknesses respond differently to tectonic forces and thermal activity, thereby influencing the thermal structure and type of basin. Under external forces or sedimentary loads, the lithosphere can fracture or bend, providing accommodation space for sedimentation. The thickness and properties of the lithosphere control the formation of sedimentary basins and are influenced by mantle convection. Previous studies have classified basins into extensional basins, cratonic basins, compressional basins (foreland basins, arc basins), and strike-slip basins based on the properties and thickness of the lithosphere, rheological boundaries within the Earth, intraplate stresses, and sedimentary loads (Fig. 14). Regardless of the type of basin, basin formation processes are inevitably constrained by the redistribution, adjustment, and movement of deep crustal and mantle materials. They are influenced by multiple tectonic events and superimposed effects, leading to uplift at the top of the upper mantle under vertical force conditions and subsequent basin formation under horizontal force conditions (Wang et al., 1998).

Extensional basins, also known as rift basins or graben basins, include intraplate rift basins and margin rift basins. In the study area, these basins are mainly distributed in eastern and southern China. They have thinner lithospheric thicknesses, significant fluctuations in lithospheric thickness and are rich in oil and gas. In eastern China, extensional movement resulted from the subduction of the Pacific Plate toward the Eurasian Plate, causing the Chinese continental crust to spread eastward, thus leading to the formation of lithosphere rupture zones in the NNE direction, with the upper mantle uplifting along zones of crustal thinning and rift zones. The local mantle uplift zones exhibited significant lithospheric thinning and high relative fluctuations. Factors, such as the subduction direction and angle of the Pacific Plate, the amplitude and thermal state of the uplifting upper mantle, and the deformation mechanism of the lithosphere, controlled the development and geological characteristics of the rift basins in the study area (Li, 1982; Tian and Shi, 2002). Due to long-term geological evolution, eastern China's basins have experienced thick sedimentary deposition, frequent lithospheric structural activity, and deep magma upwelling and heating since the Mesozoic, thus leading to the stretching and thinning of the lithosphere, creating suitable geothermal gradients and well-developed fracture systems in each basin. These conditions are conducive to the formation and migration of oil and gas. In southern China, the South China Block underwent extension under the tectonic stress of the Indochina Block and the Philippine Sea Plate. Mechanical thinning of the lithosphere occurred, and

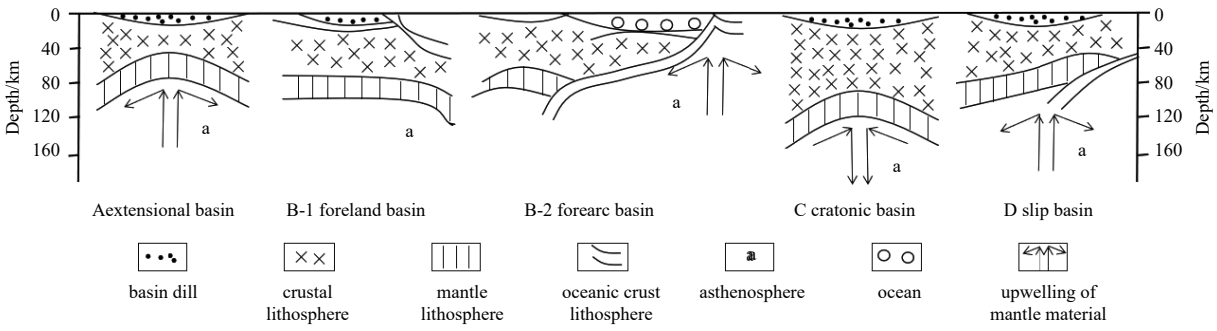

Fig. 14. Lithosphere action and basin classification models (Wang et al., 1998).

with the progression of crust–mantle interactions, asthenospheric magma continuously intruded into the lithosphere, resulting in extensive active stretching and thinning of the lithosphere. This process led to the formation of mid-ocean ridges, the subsequent development of oceanic crust basins, and continuous evolution (Ju et al., 2015).

Compressional basins, which form during the convergence of tectonic plates, include foreland basins, arc basins, and intermontane basins (Wang et al., 1998). In the study area, such basins include the Brunei-Sabah Basin and the Zengmu Basin, which are located in the southern part of the South China Sea Basin group. Compared to the oil and gas basins in the central part of the South China Sea, these basins have greater lithospheric thickness, significant relative lithospheric thickness fluctuations, and abundant oil and gas resources. During the basin formation process, the South China Block collided with the Indian–Australian Block, resulting in strong horizontal compressive stress, thus causing deformation and bending of the lithosphere, local thickening of the lithosphere, and dramatic relative fluctuations in lithospheric thickness. In the later stages, subsidence formed basins. Foreland basins are typical compressional basins, often overlying continental margin sediment wedges. They can form oil and gas accumulation zones with multiple sources and multiple layers (Ju et al., 2015). For example, the Zengmu Basin has a thick sedimentary layer and overall thick lithosphere but has noticeable relative fluctuations. It contains abundant natural gas resources.

Cratonic basins form within stable continental plates, and these relatively stable basins are rich in oil and gas resources. In the study area, such basins include foreland–craton superimposed basins and foreland–rift superimposed basins distributed in areas with thick lithosphere. The overall lithospheric thickness is high, with local thinning and moderate relative fluctuations in lithospheric thickness. Due to their relatively stable geological background and great lithospheric thickness, these basins are generally characterized by regional uplift of the upper mantle, with weak stretching and thinning of the lithosphere. The relative fluctuations in lithospheric thickness are moderate. Examples include the Sichuan Basin and the Ordos Basin. The long-term stability of the geological background in these basins leads to slow and continuous crust–mantle thermal effects. Over time, with sedimentary loading and thermal effects, they have developed well-preserved and stable oil and gas reservoirs. Therefore, in cratonic basins, a greater lithospheric thickness indicates a more stable oil and gas basin. The relative fluctuations in lithospheric thickness, along with certain degrees of uplift and subsidence, facilitate the storage and migration of oil and gas. The ancient structural belts or uplifted centers of the lithosphere often become centers of oil and gas accumulation.

Transtensional basins are closely associated with strike-slip fault systems. In the study area, these basins include the Yinggehai Basin, Zhong Jiannan Basin, Wan'an Basin, and others and are located in the gradient zone of lithospheric thickness variation. These basins have a wide range of lithospheric thickness variations, and the relative fluctuations in lithospheric thickness are also significant. These basins are Cenozoic oil and gas basins that developed in the transition zone between the Indochina Block and the South China Block. Strike-slip fault systems are well developed, and structural activity is often strong. Due to relative lateral movement between blocks, the lithosphere fractures and produces a series of faults. In these fault zones, substantial collapse deposits, debris flows, and turbidite sediments often accumulate. Additionally, some deep materials may migrate upward along fracture channels, providing favorable conditions for basin development and oil and gas generation (Wang et al., 1998; Ju et al., 2015).

In summary, the distribution of oil and gas resources may be constrained by oil and gas basins on the surface; however, this distribution is an external manifestation of the deep lithospheric thickness characteristics and structural tectonics of the basins. The thickness and relative fluctuation of the lithosphere partially reflect the geological background of the lithosphere. Different types of basins that formed under various lithospheric backgrounds exhibit significant differences in oil and gas resources. The core elements involved in the formation of different basin types are related to the upwelling of mantle magma from the deep upper mantle, an undulating lithosphere–asthenosphere boundary interface, and localized thinning of the lithosphere. Simultaneously, deep thermal substances migrate through tectonically active zones and act on large amounts of sediment, resulting in favorable conditions for oil and gas generation. Different basin types exhibit considerable diversity in their response to lithospheric thickness. The degree of variation in lithospheric thickness and relative fluctuations in basins influence the diversity in the richness of oil and gas resources within oil and gas basins. The study and discussion of the relationships between lithospheric thickness characteristics and oil and gas basin formation mechanisms presented in this paper serve as a scientific validation of the lithospheric control mechanisms proposed by previous researchers. This research provides a reference basis for exploring the tectonics of basins and the distribution patterns of oil and gas resources in China.

5 Conclusions

This study utilizes a comprehensive dataset that incorporates topographic, geoid, and geological–geophysical information such as rock layer thickness, variable rock layer density, and interface depth. Employing the principles of lithospheric isostasy theory and heat conduction, we calculate the lithospheric thickness in the China seas and adjacent areas. The lithospheric thickness exhibits notable variability across the entire region and is characterized by thicker lithosphere in continental areas with a significant range of thickness variations. There is stepped thinning and extension toward the oceanic regions, where the lithosphere is thinner and undergoes more gradual changes. Utilizing the lithospheric thickness data for the China seas and adjacent areas, we apply mathematical statistical methods to analyze two key parameters for various oil and gas basins: the minimum lithospheric thickness and the relative variation in lithospheric thickness. By combining these parameters with the abundance of oil and gas resources in the basins, we conducted a semiquantitative analysis to determine the relationships between these parameters and the abundance of oil and gas in the basins. This study reveals distinct differences in lithospheric thickness among the basins, with thicker lithosphere observed in the superimposed oil-rich basins in central China and thinner lithosphere in the oil-rich rift basins in eastern China. The variation in lithospheric thickness within basins exhibits significant disparities, notably with richer oil and gas basins demonstrating larger relative fluctuations. In the offshore basins of China, a conspicuous negative linear correlation is observed between the minimum lithospheric thickness and the relative fluctuation in lithospheric thickness. The discussion posits that the upwelling of deep thermal material induces lithospheric undulation and thinning in basins, while sustained thermal effects from deep sources create favorable conditions for hydrocarbon generation in basin sediments. The research find-

ings contribute valuable insights into the quantitative relationship between deep lithospheric structure and oil and gas basins, providing guidance for the strategic selection of future oil and gas exploration targets.

Acknowledgements

Thank you for the amendments proposed by the paper review experts. We also thank the editors for the processing and modification of the paper.

References

Afonso J C, Ben-Mansour W, O'Reilly S Y, et al. 2022. Thermochemical structure and evolution of cratonic lithosphere in Central and Southern Africa. Nature Geoscience, 15(5): 405–410, doi: 10.1038/s41561-022-00929-y

Chen Jianwen, Liang Jie, Zhang Yinguo, et al. 2019. Regional evaluation of oil and gas resources in offshore China and exploration of marine Paleo-Mesozoic oil and gas in the Yellow Sea and East China Sea. Marine Geology & Quaternary Geology (in Chinese), 39(6): 1–29

Dai Jinxing, Ni Yunyan, Liu Quanyou, et al. 2021. Sichuan super gas basin in southwest China. Petroleum Exploration and Development (in Chinese), 48(6): 1081–1088

Fullea J, Fernàndez M, Zeyen H, et al. 2007. A rapid method to map the crustal and lithospheric thickness using elevation, geoid anomaly and thermal analysis. Application to the Gibraltar Arc System, Atlas Mountains and adjacent zones. Tectonophysics, 430(1–4): 97–117, doi: 10.1016/j.tecto.2006.11.003

He Dengfa, Jia Chengzao, Tong Xiaoguang, et al. 2004. Advances in studies of petroliferous structures and tectonics. Petroleum Exploration and Development (in Chinese), 31(5): 1–7

Jin Zhijun, Yin Jinyin, Xie Fangke, et al. 2003. Lithosphere structures, petroleum accumulation and distribution in petroliferous basin. Chinese Journal of Geology (in Chinese), 38(3): 392–402

Ju Yiwen, Sun Ying, Wang Guochang, et al. 2015. Dynamic types of basin formation and evolution and its geodynamic mechanisms. Chinese Journal of Geology (in Chinese), 50(2): 503–523

Kang Yuzhu, Xing Shuwen, Li Huijun, et al. 2019. Features of structural systems in northern China and its control on basin and hydrocarbon distribution. Journal of Geomechanics (in Chinese), 25(6): 1013–1024

Lachenbruch A H, Morgan P. 1990. Continental extension, magmatism and elevation; Formal relations and rules of thumb. Tectonophysics, 174(1–2): 39–62, doi: 10.1016/0040-1951(90)90383-J

Laske G, Masters G, Ma Z, et al. 2012. CRUST1.0: An updated global model of Earth's crust. In: EGU General Assembly 2012. Vienna: EGU, 3743

Li Desheng. 1982. Tectonic types of oil and gas basins in China. Acta Petrolei Sinica (in Chinese), (3): 1–12

Li Sidian. 2015. Advancement, trend and new challenges in basin geodynamics. Earth Science Frontiers (in Chinese), 22(1): 1–8

Li Mengkui, Song Xiaodong, Li Jiangtao, et al. 2018a. Lithospheric structures of the main basins in Mainland China and its tectonic implications. Earth Science (in Chinese), 43(10): 3362–3372

Li Sanzhong, Suo Yanhui, Li Xiyao, et al. 2018b. Mesozoic plate subduction in West Pacific and tectono-magmatic response in the East Asian ocean-continent connection zone. Chinese Science Bulletin (in Chinese), 63(16): 1550–1593, doi: 10.1360/N972017-01113

McKenzie D. 1977. Surface deformation, gravity anomalies and convection. Geophysical Journal International, 48(2): 211–238, doi: 10.1111/j.1365-246X.1977.tb01297.x

Parsons B, Sclater J G. 1977. An analysis of the variation of ocean floor bathymetry and heat flow with age. Journal of Geophysical Research, 82(5): 803–827, doi: 10.1029/JB082i005p00803

Pavlis N K, Holmes S A, Kenyon S C, et al. 2012. The development and evaluation of the Earth Gravitational Model 2008 (EGM2008). Journal of Geophysical Research: Solid Earth, 117(B4): B04406

Sandwell D T, Müller R D, Smith W H F, et al. 2014. New global marine gravity model from CryoSat-2 and Jason-1 reveals buried tectonic structure. Science, 346(6205): 65–67, doi: 10.1126/science.1258213

Straume E O, Gaina C, Medvedev S, et al. 2019. GlobSed: updated total sediment thickness in the World's oceans. Geochemistry, Geophysics, Geosystems, 20(4): 1756–1772

Tian Zaiyi, Shi Buqing. 2002. Geological features and petroleum reservoir formation in meso-cenozoic sedimentary basins in China. Geotectonica et Metallogenia (in Chinese), 26(1): 1–5

Wang Dongpo, Liu Li, Xue Linfu, et al. 1998. Geodynamic mechanisms for the formation of sedimentary basins and their classification. Sedimentary Facies and Palaeogeography (in Chinese), 18(3): 7–13

Xie Yuhong, Gao Yangdong. 2020. Recent domestic exploration progress and direction of CNOOC. China Petroleum Exploration (in Chinese), 25(1): 20–30

Xu Changfang. 2003. The study of lithospheric tectonics and basin formation of Chinese Mainland and migration of oil and gas. Earth Science Frontiers (in Chinese), 10(3): 115–127

Xu Ya, Zeyen H, Hao Tianyao, et al. 2016. Lithospheric structure of the North China Craton: integrated gravity, geoid and topography data. Gondwana Research, 34: 315–323, doi: 10.1016/j.gr.2015.03.010

Zeyen H, Fernàndez M. 1994. Integrated lithospheric modeling combining thermal, gravity, and local isostasy analysis: application to the NE Spanish Geotransect. Journal of Geophysical Research: Solid Earth, 99(B9): 18089–18102, doi: 10.1029/94JB00898

Zhang Gongcheng, Qu Hongjun, Liu Shixiang, et al. 2015. Tectonic cycle of marginal sea controlled the hydrocarbon accumulation in deep-water areas of South China Sea. Acta Petrolei Sinica (in Chinese), 36(5): 533–545

Zhang Yimi, Wang Wanyin, Li Linzhi, et al. 2023. Influence of the Moho surface distribution on the oil and gas basins in China seas and adjacent areas. Acta Oceanologica Sinica, 42(3): 167–188, doi: 10.1007/s13131-022-2136-8

Zhang Gongcheng, Zhu Weilin, Mi Lijun, et al. 2010. The theory of hydrocarbon Genernation controlled by source rock and heat from circle distribution of outside-oil fields and inside-gas fields in South China Sea. Acta Sedimentologica Sinica (in Chinese), 28(5): 987–1005

Zheng Min, Li Jianzhong, Wu Xiaozhi, et al. 2019. Potential of oil and natural gas resources of main hydrocarbon-bearing basins and key exploration fields in China. Earth Science (in Chinese), 44(3): 833–847

Zhu Rixiang, Zhang Shuichang, Wan Bo, et al. 2023. Effects of Neo-Tethyan evolution on the petroleum system of Persian Gulf superbasin. Petroleum Exploration and Development, 50(1): 1–13, doi: 10.1016/S1876-3804(22)60365-3

Zhu Weilin, Wu Jingfu, Zhang Gongcheng, et al. 2015. Discrepancy tectonic evolution and petroleum exploration in China offshore Cenozoic basins. Earth Science Frontiers (in Chinese), 22(01): 88–101.